Pergamon

Journal of Structural Geology, Vol. 16, No. 8, pp. 1041 to 1059, 1994

0191-8141/94 $07.00+0.00

Drainage systems and the development of normal faults: an example from Pleasant Valley, Nevada

JAMES JACKSON

Bullard Laboratories, Madingley Road, Cambridge CB3 0EZ, U.K.

and

MIKE LEEDER

Department of Earth Sciences, University of Leeds, Leeds LS2 9JT, U.K.

(*Received* 14 *August* 1992; *accepted in revised form* 27 *September* 1993)

Abstract—Drainage systems in regions of active extension contain information about fault zone structure and development, and particularly about the lateral growth of individual fault segments, that is difficult to obtain by more conventional means such as the dating of sedimentary material. We investigate drainage-fault interaction in Pleasant Valley, Nevada, where a large normal-faulting earthquake occurred in 1915. We find geomorphological evidence for a propagation (increase in length) of several km at both ends of one of the 1915 fault segments. At one end we estimate the propagation rate to be about 50 m per earthquake. This estimate is uncertain, but is within the range predicted by theoretical models of fault growth. Drainage along the axes of half graben in this region may be influenced by the spacing of tilted fault blocks: the highest valleys are also the narrowest. Whether the axial streams succeed in reaching lower neighbouring sinks depends on whether sedimentation rates are able to keep basins filled to the levels of the basement highs that separate half graben of opposite polarity. A knowledge of modern drainage–fault interactions may help predict drainage systems and the position of potential syn-rift reservoir sediments in older extensional terrains where fault configurations (but not facies distributions) are known from seismic reflection surveys.

INTRODUCTION

IN THIS paper we examine the relationship between drainage patterns and fault geometry in a region of active continental extension. There are two reasons for this study: (i) the drainage may contain information about the fault development and growth that is difficult to obtain by other methods; and (ii) it may help to interpret syn-rift sedimentation and facies in older graben systems, where the faults have been mapped from seismic reflection profiles but the sediments are poorly known.

Extensional half-graben systems on the continents are often longer than 100 km, but are seldom bounded by continuous normal faults. Instead, the faults typically occur in segments that step en échelon or change the polarity of their dip along strike. The observation that normal faulting earthquakes on the continents are rarely larger than M_s ~6.5–7.0 (Jackson & White 1989) suggests that there is an upper limit to the fault segment length, which controls the maximum extent of rupture and hence earthquake size. Jackson & White (1989) suggest that the maximum segment length is typically in the region of 20 km, which would generate an earthquake of M_w ~6.5 (Shimazaki 1986). Those normal faulting earthquakes this century with larger magnitudes (up to M_w ~7.2) can be shown to be multiple events that involved sequential rupture on two or more such segments (see Jackson & White 1989). A maximum segment length of ~20 km is supported in a general way by geomorphological observations of the continuity of range fronts (e.g. Jackson & White 1989, Wallace 1989, Crone & Haller 1991, Roberts & Jackson 1991), but segment boundaries cannot always be precisely defined or identified in this way and some segment lengths may be longer (e.g. De Polo *et al.* 1991, Machette *et al.* 1991). It is possible that the commonly observed maximum segment length of ~20 km is related to the thickness of the upper seismogenic layer of the crust (Jackson & White 1989), which is typically about 15 km, or to the maximum down-dip width of the fault within the seismogenic layer (Wallace 1989). In the oceans, where the seismogenic thickness can be as great as 40 km, normal faulting earthquakes seaward of trenches reach magnitudes of $M_w > 8.0$ and involve rupture on faults with total lengths of several hundred km.

The structure and evolution of regions where fault segments terminate are of great significance in seismology, tectonics, sedimentology and geomorphology. Recent attention has focussed on the observation that such sites are often where rupture initiates or terminates in earthquakes (e.g. Fonseca 1988, Schwartz & Sibson 1989, De Polo *et al.* 1991, Zhang *et al.* 1991). Aftershocks of large earthquakes often concentrate near such terminations, and are usually distributed throughout a deforming volume between fault segments, attesting to pervasive small scale deformation (e.g. Lyon-Caen *et al.* 1988) which can sometimes be seen at the surface (e.g. Jackson *et al.* 1982, Susong *et al.* 1990). The vertical movements and tilting associated with normal faults

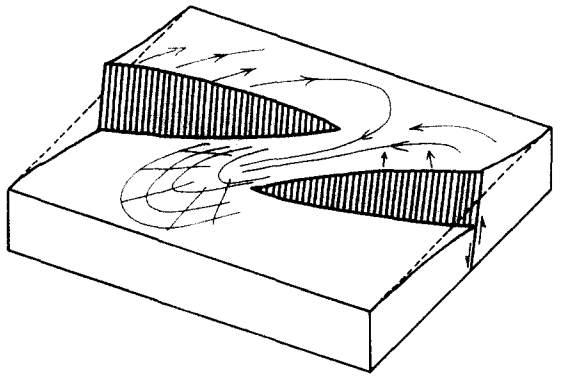

Fig. 1. Idealized sketch illustrating a large stream system that enters a graben through a step in the bounding normal fault segments. These streams exploit the natural slope parallel to strike that exists in the en échelon step, as they flow from the footwall of one fault into the hanging wall of the other. The sketch does not include the often smaller catchments that drain the fault directly, and is not drawn to scale, though the offset between fault segments is typically 1–10 km.

establish drainage patterns that are strongly influenced by the continuity of the faulting itself: large alluvial fans and fan deltas are often located between offset fault segments (Fig. 1), since the drainage basins in the footwall hinterlands that feed them are usually much larger than those responsible for material derived directly from the fault-bounded range front (e.g. Leeder & Gawthorpe 1987, Roberts & Jackson 1991, Leeder & Jackson 1993). In older inactive basins, such as the North Sea, such fans are potential hydrocarbon reservoirs (Harris & Fowler 1987), so an understanding of their distribution and evolution is of economic importance. Roberts & Jackson (1991) and Leeder *et al.* (1991) examined the drainage patterns associated with active normal faults in Greece. Their studies emphasized the two main controls on drainage in that region: the strength of the rocks in the footwalls and the lateral continuity of the fault segments.

Offsets between fault segments are usually considered as static structures: but they must change with time if the fault segments grow or decay along strike. Two observations require faults to increase their displacement with time: (i) the ratio of total displacement to length on geological faults is typically in the range 10^{-3}–10^{-1}; yet (ii) the ratio of the slip to rupture length in an earthquake is much smaller, typically 10^{-5}–10^{-4} (Scholz *et al.* 1986, Watterson 1986). The first observation suggests that faults also grow in length with time. If some faults grow, then in order to maintain the earthquake frequency–magnitude relation describing the relative abundance of small to large faults that are active at any one time, other faults must die or decrease their active lengths (see Walsh & Watterson 1992). The geometry in Fig. 1 could evolve in various ways: the faults could simply grow *in situ*, increasing displacement without changing length; they could be growing towards each other; or one could be growing at the expense of the other. We would like to know how such discontinuities evolve with time, but only in exceptional circumstances (e.g. Ebinger 1989) are we likely to be able to constrain this by conventional geological techniques, as material available for dating in these continental, often erosional, environments is so scarce.

In order to look at footwall drainage associated with active normal fault systems in continental interiors, away from the influence of dramatic base level changes associated with Pleistocene sea level fluctuations, we chose the Basin and Range Province of the western U.S.A. In particular, we focussed on the Central Nevada Seismic Belt in which a number of large normal-faulting earthquakes produced surface rupture this century, including the 1915 Pleasant Valley earthquake (Fig. 2). The historical and Quaternary faults in this area have been mapped in detail by Wallace (1977, 1978a,b, 1984a) and Wallace & Whitney (1984). Our purpose is to examine the drainage systems in relation to this faulting, particularly in Pleasant Valley.

GENERAL FEATURES OF THE DRAINAGE

This paper is mainly concerned with the effects of surface deformation and faulting on stream channel behaviour, and particularly on whether net incision or deposition is taking place. However, other factors, including footwall rock type, climate and base level changes can also have a strong influence on drainage, and it is important that these other effects are isolated.

The footwall rocks in this part of Nevada are mostly quartzites, carbonates and igneous rocks of Cambrian to Triassic age, with some additional Tertiary lacustrine sediments and volcanic rocks. Most are relatively competent, and rock type does not greatly influence the morphology of the fault scarp at the surface (Fonseca 1988). The influence of rock type on the size of drainage basins can be more pronounced, and is discussed below and in Leeder & Jackson (1993).

Pleistocene and Holocene climatic variations have caused stream channels to incise or aggrade by varying the amount of run-off or sediment supply from catchment slopes (see e.g. Dohrenwend 1987). Since our principle interest was the degree to which footwall-derived alluvial fans and streams were incised, we could estimate the importance of climatic effects by comparing fan systems close to and far from active faults. Large-scale incision (i.e. by tens of metres) of footwall-derived fans or bajadas occurs only when they are cut by faults (e.g. Fig. 3) or are adjacent to areas that have suffered dramatic base level changes. Local fan head incision (of a few metres), probably caused by peak discharges after occasional storms, is quite common regardless of structural position. For our purposes, the most significant effect of changing climate is the fluctuation in lake levels in the region. During the Quaternary north-central Nevada contained numerous lakes, whose levels fluctuated in response to changing climatic conditions. The Humboldt River and Buena Vista valleys were filled by Lake Lahontan, and Dixie Valley was occupied by a separate lake. The high stands of these lakes occurred about 12,000 years ago (e.g. Morrison 1964, Miflin & Wheat 1979, Benson & Thompson 1987) and they left

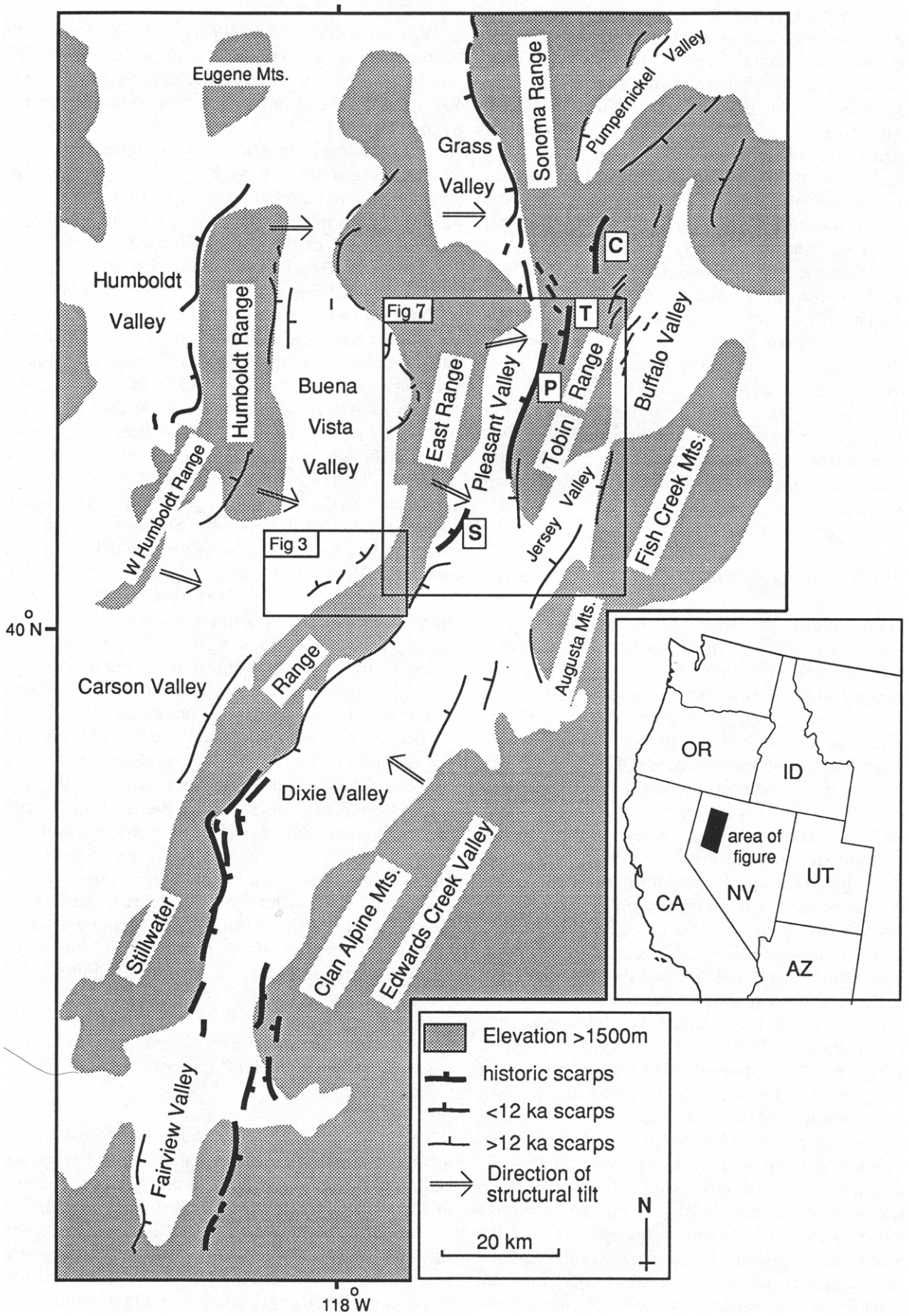

Fig. 2. Location map of the Central Nevada Seismic Belt. The regions covered by Figs. 3 and 7 are shown by boxes. S, P, T and C are the Sou Hills, Pearce, Tobin and China Mountain fault segments that moved in the 1915 Pleasant Valley earthquake. Faults are based mainly on work by Slemmons (1957), Wallace (1978b, 1984a) and Wallace & Whitney (1984).

many shorelines as their levels declined (Fig. 3). These base level changes could potentially have influenced drainage by causing the establishment and incision of streams that would then have been unable to migrate in response to tilting or changes in the configuration of faulting. However, in Buena Vista Valley and Dixie Valley the shoreline slopes were low and are only incised where they coincide with faults (Fig. 3), presumably because changes in base level had little effect on stream power. This was also the conclusion of Wallace (personal communication), and is implicit in some of his work (see Fig. 3 and Wallace 1977).

Alluvial fans are commonly incised in the footwalls of faults and we conclude that the degree of incision is controlled mainly by structural position relative to faults rather than by climate or rock type. In contrast to the incised footwalls, the hanging walls of faults are generally observed to be areas of deposition (Fig. 3). The exceptions to this rule were local fan head incision caused by storm outwash, and two localities (which we shall discuss below) in Pleasant Valley where incision continued across the fault well into the downthrown hanging wall.

GENERAL SETTING OF PLEASANT VALLEY

Pleasant Valley is a N–S half graben about 50 km long, bounded on its east side by the Tobin Range and a system of normal faults that dip to the west (Fig. 2). Most of the drainage basins in the steep footwalls of this fault system are relatively small, whereas larger palmate basins characterize the gentler slopes of the hanging wall in the East Range on the western side of Pleasant Valley (Fig. 7). The fault system on the east side of Pleasant Valley was activated by an earthquake in 1915 that ruptured the surface along four segments in an en échelon right-stepping pattern over a total distance of ~60 km, with average displacements in the region of 2–3 m (Wallace 1984a). The four segments are, from south to north: the Sou Hills, the Pearce, the Tobin and the China Mountain faults (Fig. 2). The few seismograms available for this earthquake suggest that it consisted of several discrete sub-events (Doser 1988); an inference that is consistent with the segmented fault scarps seen at the surface. Pleasant Valley is in a part of the Basin and Range Province that is dominated by faults dipping west and a regional tilting of Tertiary rocks to the east (Stewart 1980a,b). We will first discuss the southern end of Pleasant Valley, which is separated along strike from Dixie Valley, a half graben of the opposite polarity, by the Sou Hills. A discontinuous scarp about 8 km long on the west side of the Sou Hills was the southernmost segment of substantial faulting in the 1915 earthquake (Wallace 1984a). The Sou Hills may be part of a regional E–W-trending narrow belt that separates domains with different tilt directions (Stewart 1980a, Fonseca 1988, Thenhaus & Barnhard 1989). We then discuss the northern end of Pleasant Valley, where the geomorphology contains the clearest evidence of fault propagation.

PLEASANT VALLEY: SOUTHERN END

The southern part of the Pleasant Valley fault system is shown in Fig. 4. The Pearce fault, which is the central and longest of the four fault segments that moved in 1915, follows the abrupt edge of the Tobin Range front for much of its length and dies away in the south as the range front loses elevation. The southern end of the Pearce fault segment partially overlaps an older fault segment situated 2.5 km farther east (marked F in Figs. 4a and 7) and which also dips west. The topographic step in the footwall of the Pearce fault coincides with the emergence of Wood Canyon into Pleasant Valley. The 1915 surface ruptures on the Pearce fault continue 4–5 km south of Wood Canyon, but become discontinuous, smaller in offset, and distributed over an area 3 km wide. The northern end of the 1915 Sou Hills scarp begins near the southern end of the Pearce scarp, but is situated 4 km to the west. The Sou Hills form a basement high separating Pleasant Valley from Dixie Valley to the south. Fonseca (1988) points out that the elevations of the Tobin, Stillwater and East Ranges all decrease towards the latitude of the Sou Hills (Figs. 5 and 8). Between the Pearce and Sou Hills scarps lies Spring Creek, the axial drainage stream of Pleasant Valley, which flows south into Dixie Valley.

There are two anomalous features of the drainage in the southern part of Pleasant Valley that require explanation, related to Wood Canyon and Spring Creek. Wood Canyon is by far the most dramatic canyon to discharge across the southern end of the Pearce scarp, and is the only canyon that has incised across the hanging wall, from the scarp to the axial stream of Spring Creek (Figs. 4 and 5). The presence of a large stream in the step between the two fault segments that bound the Tobin Range front is not a surprise (see Fig. 1), but its incision into the hanging wall of the fault is clearly anomalous, as most streams show incision only in the footwalls (e.g. Fig. 3). Spring Creek is anomalous because it flows *south* as an axial stream between the Pearce and Sou Hills scarps, whereas the natural slope generated by the faulting would dip north, passing from the uplifted footwall of the Sou Hills fault to the subsiding hanging wall of the Pearce fault.

Spring Creek, the Sou Hills and the origin of transverse basement ridges where fault systems change their polarity of dip

The Sou Hills occupy an important structural position in a region where the polarity of the major normal faults changes from W-dipping in Pleasant Valley to E-dipping in Dixie Valley. The Sou Hills themselves consist of Tertiary lake sediments and volcanic rocks, generally tilted to the east (Nosker 1981). The fact that they occupy a region towards which the elevations of the Stillwater, Tobin and East Ranges decrease and the depths of half graben in Dixie and Pleasant Valleys become shallower, suggests that the displacements on the major range-bounding faults also decrease (Figs. 5 and 8)

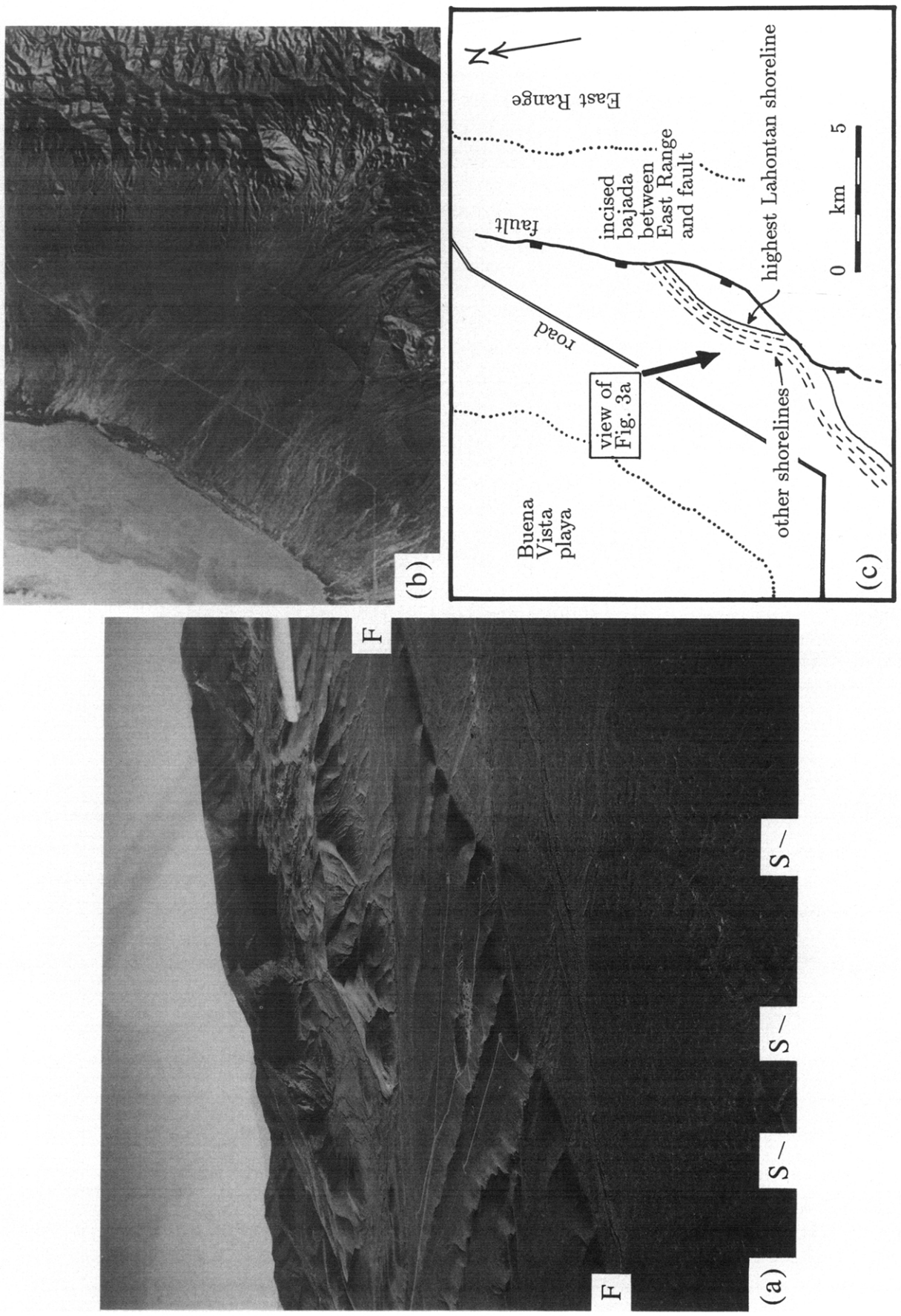

Fig. 3. Faults and shorelines in Buena Vista Valley. (a) Oblique air photograph of a fault on the northwest flank of the Stillwater Range, by Kitten Springs (see Fig. 2 for location). The prominent scarp (F) with incised drainage in the uplifted bajada of the footwall is a fault, which is eroded back in its southern (right) part by Lake Lahontan shorelines (S) that form the subdued scarps in the foreground. The shorelines are not incised on their higher sides, except where they coincide with the fault. Note the post high stand deposition in the hanging wall of the fault which has locally obscured traces of the shoreline terraces. View is to the southeast. Photograph by R. E. Wallace. (b) LANDSAT image of the part Buena Vista Valley shown in (a). See Fig. 2 for location. (c) Sketch map of the region covered in (b).

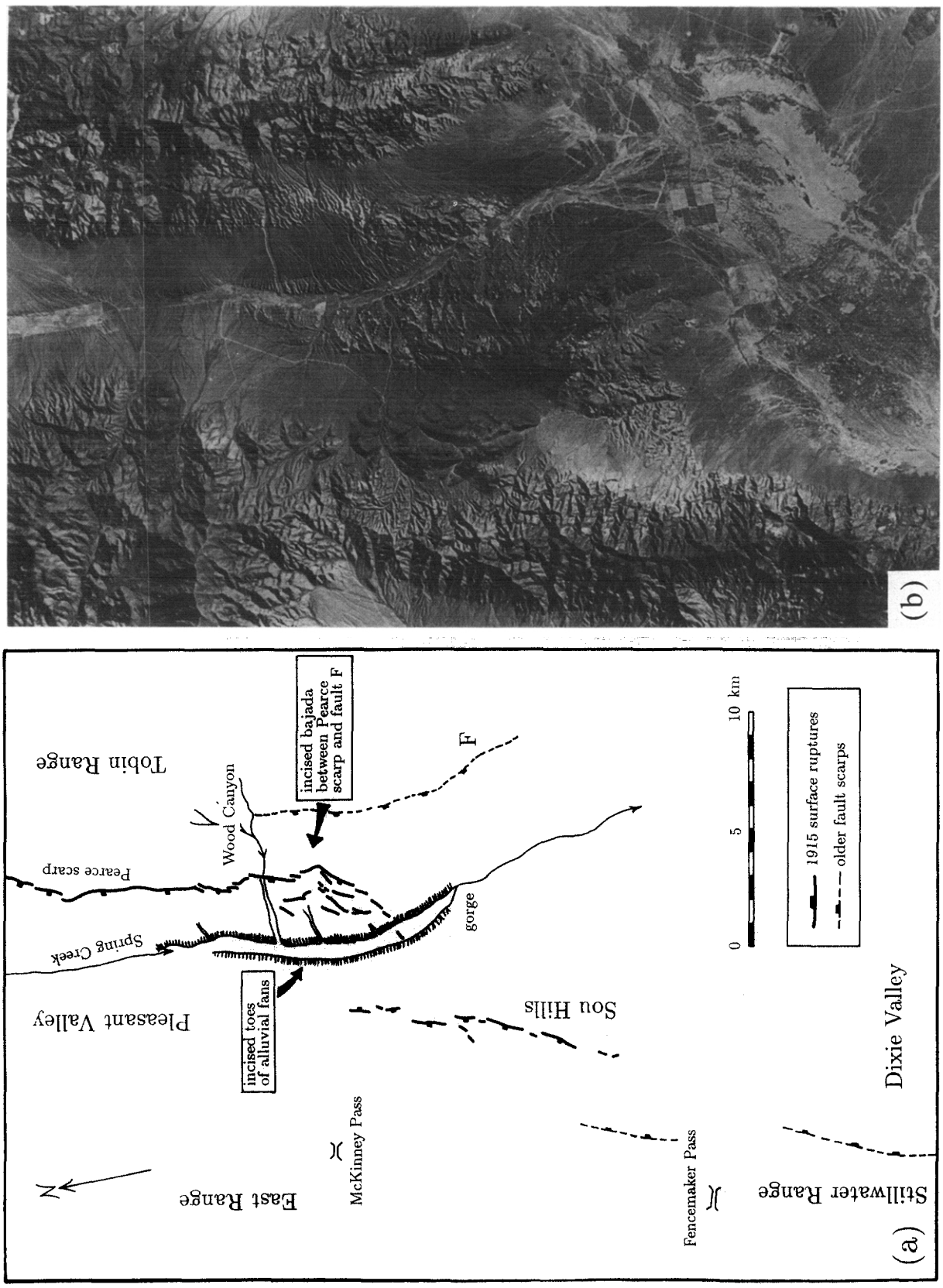

Fig. 4. (a) Map of the southern end of Pleasant Valley, illustrating the principal features in (b). (b) LANDSAT image of southern end Pleasant Valley, covering the area in (a).

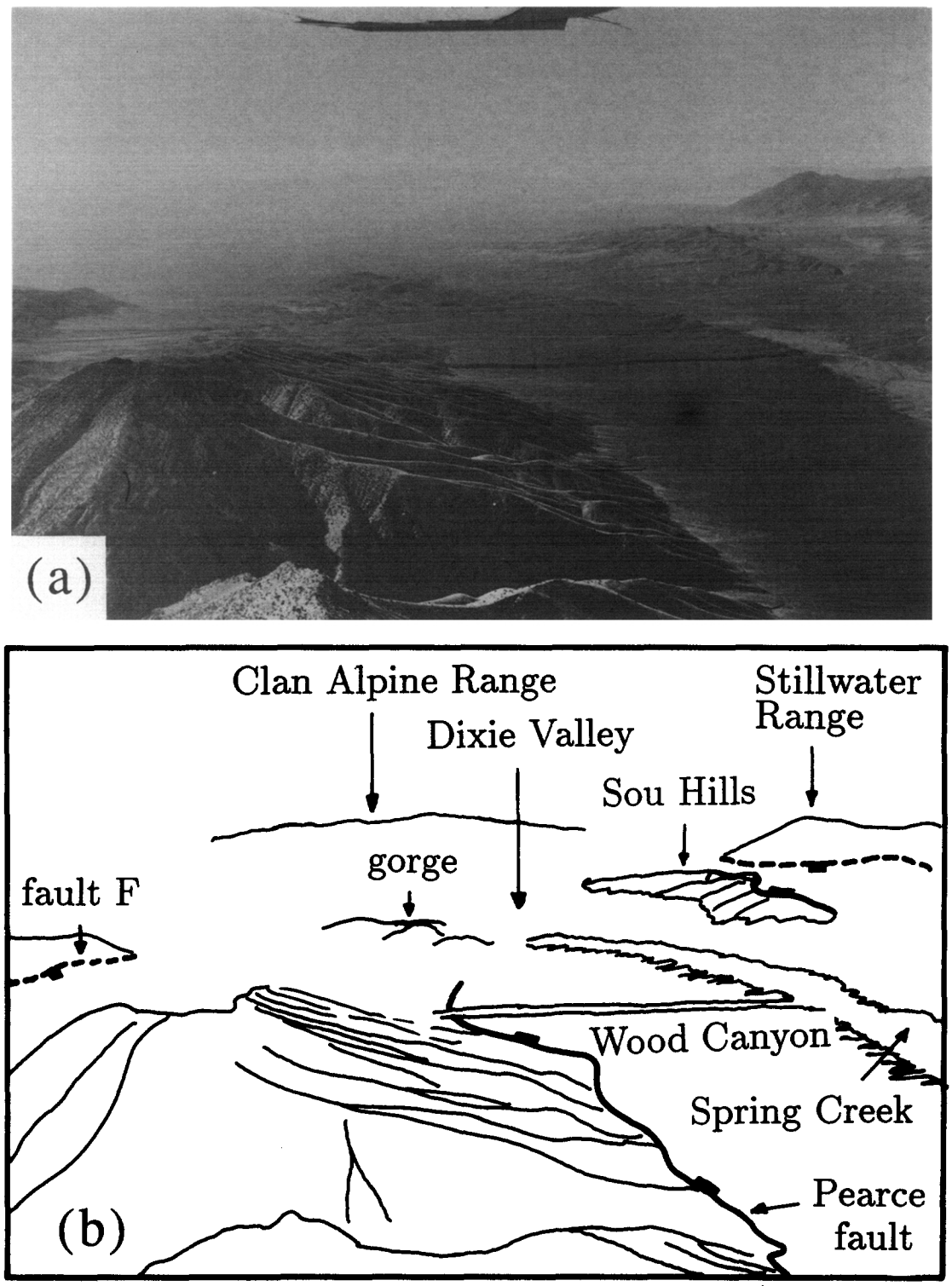

Fig. 5. (a) Oblique air photograph and (b) a sketch looking south over the southern end of Pleasant Valley. Notice the gradual loss of elevation of the footwall of the Pearce fault segment, the incised course of Wood Canyon, and the incised toes of the alluvial fans bordering Spring Creek (see also Fig. 4).

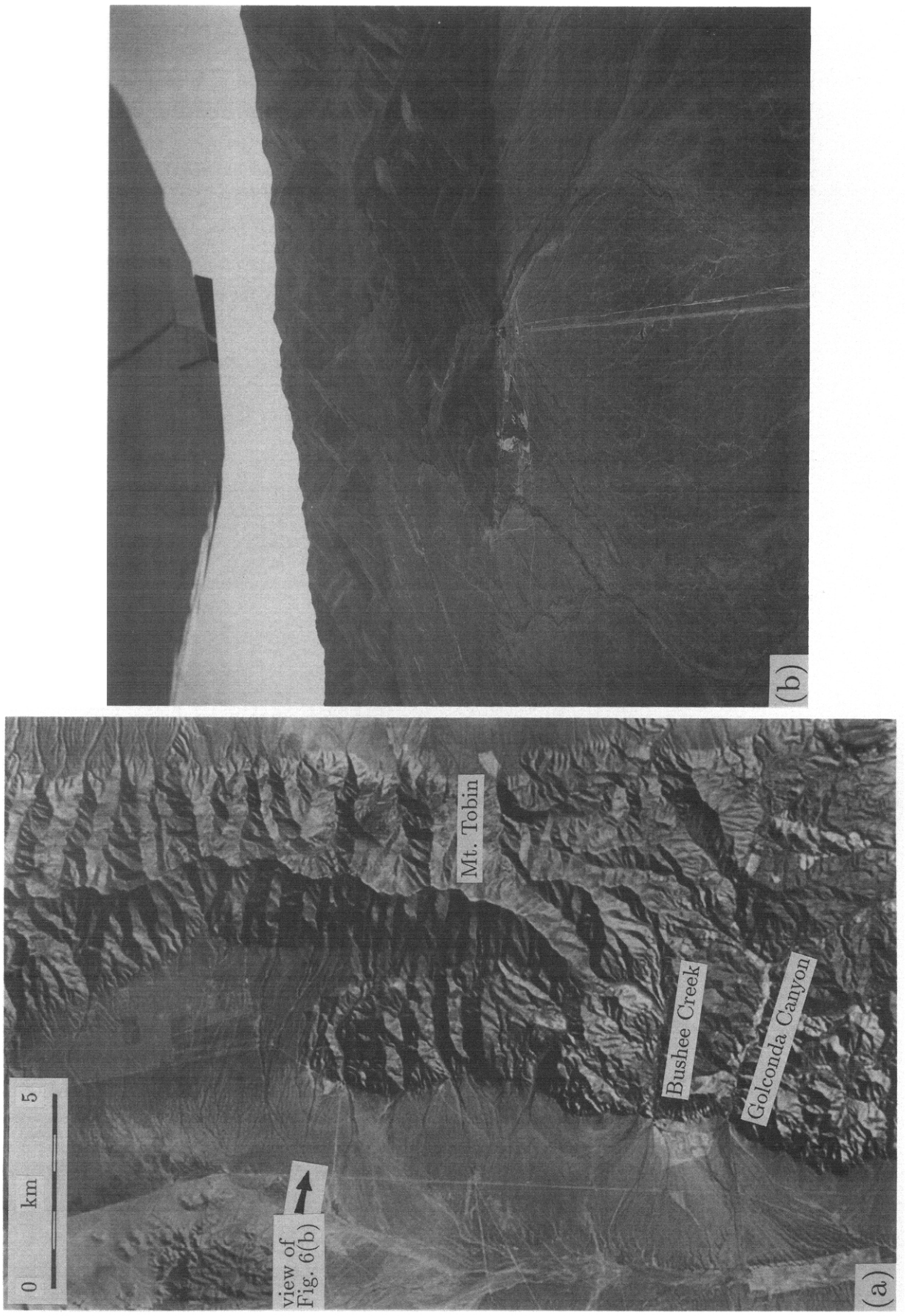

Fig. 6. (a) Satellite image of northern Pleasant Valley, showing the overlap between the Pearce and Tobin fault segments. (b) Oblique air photograph looking east over Pearce–Tobin overlap zone (see a for location). The straight road in the foreground leads to the Siard Ranch, on the Pearce scarp at the mouth of Shell Canyon (stream D in Fig. 10b). Note the flat bottom to the incised channel of the stream issuing from Shell Canyon (D) in the hanging wall of the Pearce fault. Compare with the sketch in Fig. 13. Photograph by R. E. Wallace.

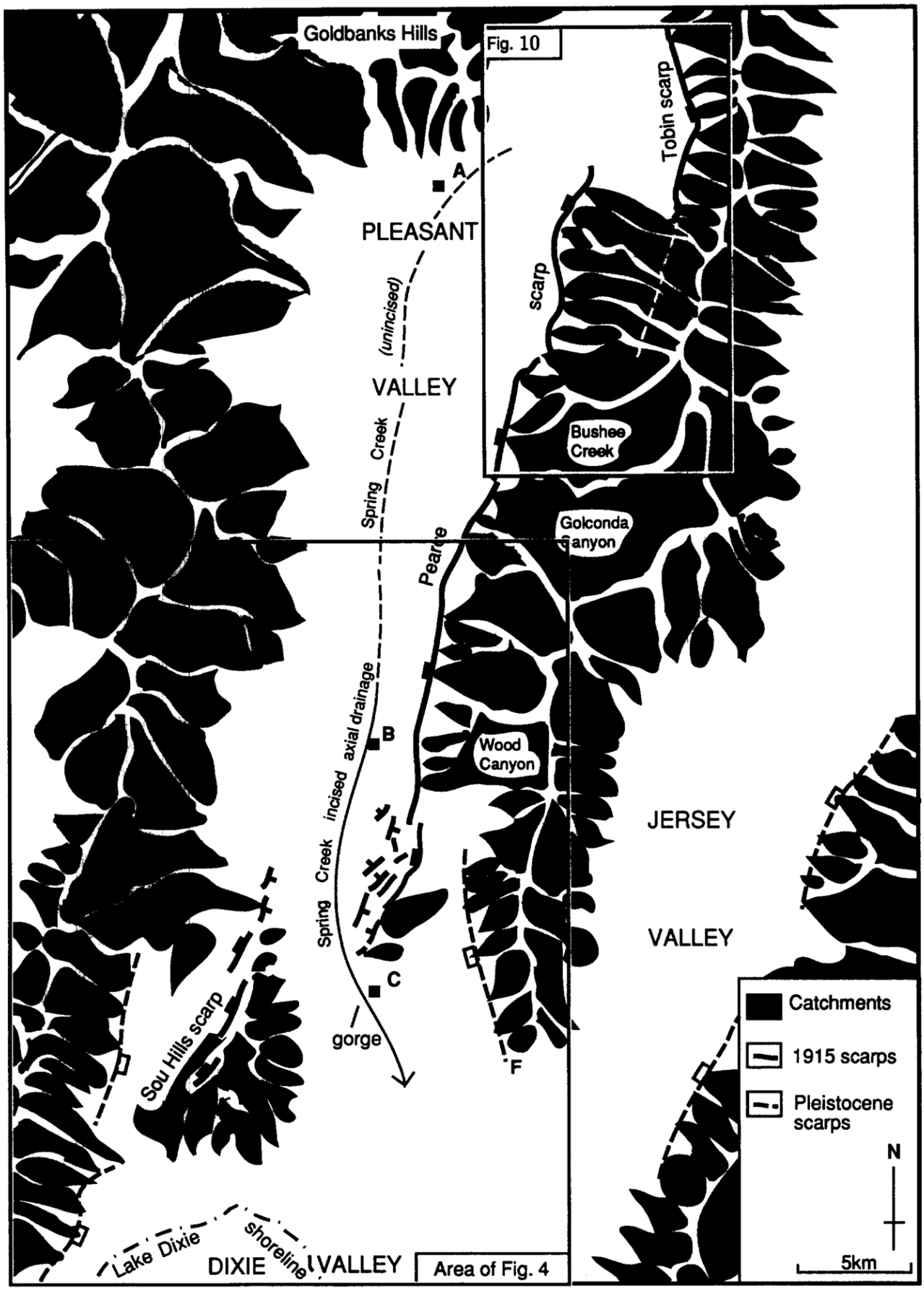

Fig. 7. Map of the drainage basins in Pleasant Valley (see Fig. 2 for location). Catchments in the ranges are shown in black, with their intervening divides in white. The course of the axial stream, Spring Creek, is shown dashed where it is not incised, and solid where it flows in a previously incised valley that is now depositional (see text).

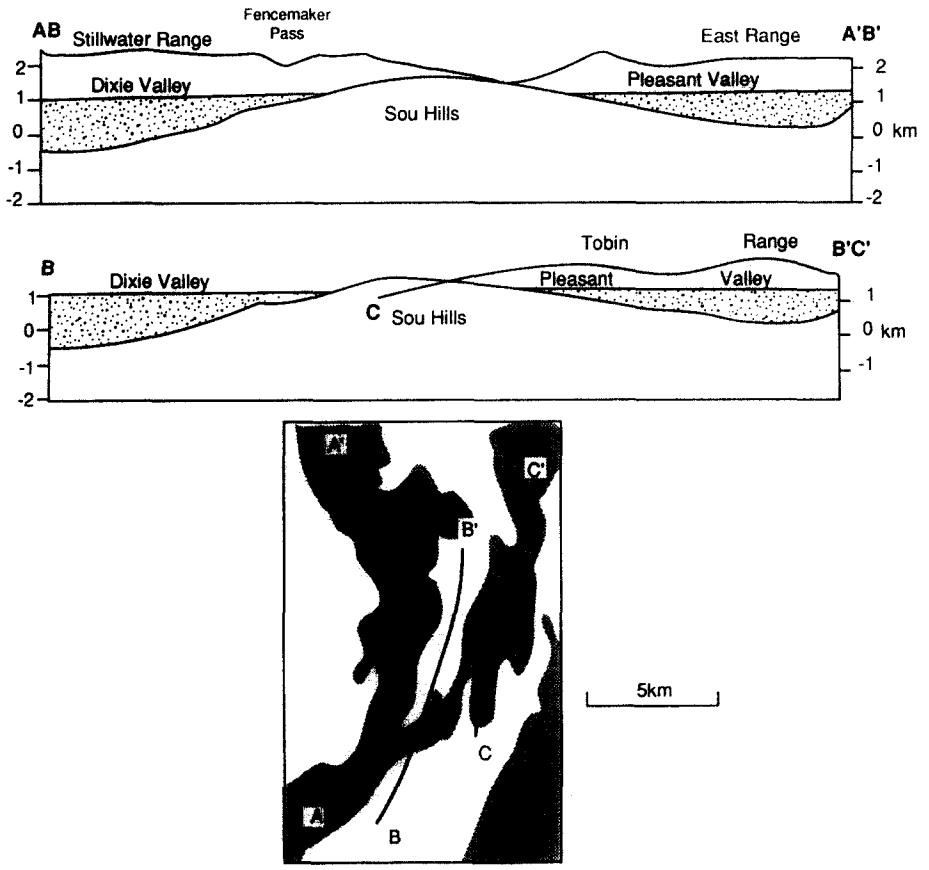

Fig. 8. Topographic profiles along the East Range, Tobin Range and Stillwater Range, and thicknesses of valley fill sediments (estimated from gravity measurements), showing that both these decrease towards the Sou Hills (adapted from Fonseca 1988).

(Fonseca 1988). Transverse intra-basin highs of this sort are commonly located near segment offsets in range-bounding faults (e.g. Wheeler 1989, Crone & Haller 1991) or where a half graben system changes polarity along strike (e.g. Rosendahl *et al.* 1986, Ebinger 1989). It is probable that displacement on the major range-bounding faults decreases towards such regions (Fonseca 1988, Wheeler 1989, Crone & Haller 1991). We suspect that as the displacement dies out, the depth to which the fault penetrates becomes shallower (see e.g. Gibson *et al.* 1989), and that this allows the ends of major faults with opposing dip to overlap at the surface without intersecting at depth (Fig. 9a). Yet we doubt whether there is a significant difference between the amount of *regional* extension at the latitude of the Sou Hills and that to the north in Pleasant Valley or to the south in Dixie Valley. In other words, in the region of the basement high the slip deficit on the major faults must be made up on other smaller faults. The southern end of the Pearce scarp splays into a series of minor faults, and the 1915 Sou Hills scarp is just one of at least four to six relatively minor scarp-bounding faults at that latitude over a width of about 25 km (Figs. 4 and 7). This contrasts with central Pleasant Valley, bounded by the much higher range front along the Pearce scarp, where the next significant fault to the west is along the western side of the East Range in Buena Vista Valley, ~25 km away (Fig. 2).

The increased density of faulting at the ends of fault segments and where half graben systems change polarity is likely to influence the vertical motions that accompany the faulting. In a region of simple large half graben structures the depths of basins and elevations of the main ranges are controlled largely by tilting and fault spacing (Jackson *et al.* 1988, Yielding 1990). In the simplest model of all, in which the fault-bounded blocks of present dip θ rotate like dominoes, the amount of extension (β) is related directly to the tilting (ϕ), since $\beta = \sin(\theta + \phi)/\sin\theta$ (see e.g. Jackson & McKenzie 1983). The total elevation between crest and trough of the half graben is $h = (W \sin\phi)/\beta$, where W is the current horizontal spacing between the faults. The crests and troughs are a height $h/2$ above and below the average topographic level, which should be the same everywhere for regions of equal extension. These relations are illustrated in Fig. 9(b). Where the faults are closely spaced, the heights of the crests and troughs above and below the average level are much less than if the faults are widely spaced. If, therefore, segment offsets and accommodation zones achieve the same extension as their adjacent major half graben, but do so by more closely spaced faults, we would expect these zones to form transverse basement highs (or ridge crest lows). The size of this effect is easily calculated. As an illustration, let us assume that the faults dip at 45° (Doser 1986, Doser & Smith 1989) and that the tilt

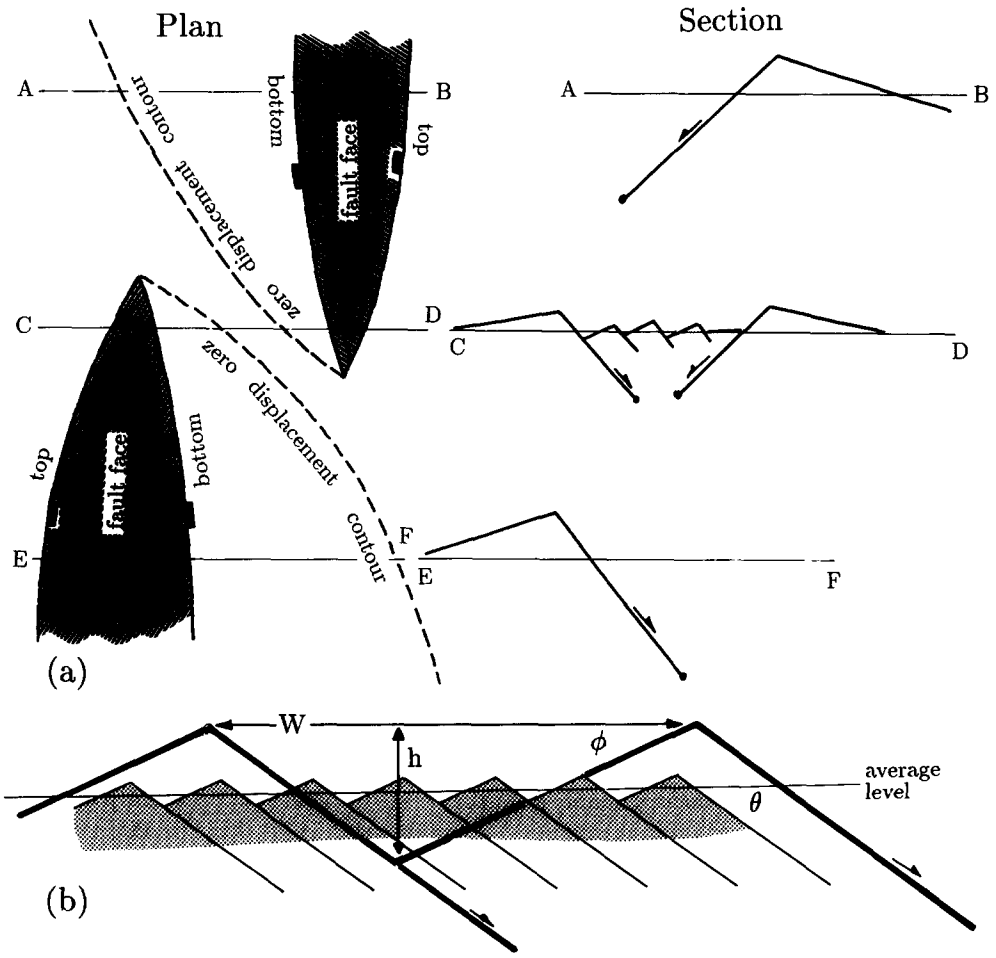

Fig. 9. (a) On the left is a plan view showing faults of opposing dip getting shallower towards their ends in a region where the half-graben polarity changes. The projection of the zero displacement contour to the surface is shown by dashed lines. On the right is a cross-section through the region of overlap (C–D), showing that because the faults are shallow they do not intersect at depth. Their depth penetration increases as their displacement increases away from their terminations (sections A–B and E–F). (b) Cross-sections illustrating the idealized saw-tooth topography associated with rotating faults, showing that for a given extension (i.e. amount of tilting) the amplitude is smaller for small fault spacing (thin lines) than for the large fault spacing (thick lines); see text. θ is the present fault dip, ϕ is the amount of tilting. W (the present fault spacing) and h (the crest-to-trough amplitude) are identified for the wide blocks.

associated with this faulting is 10° (a common dip for the Tertiary basalts in the region). The extension, β, is then 1.16. The crest-to-trough height, h, is then ~700 m if $W = 5$ km (Sou Hills), or ~3500 m if $W = 25$ km (central Pleasant Valley). The height of the basement ridge would thus be ~350 m above the average level compared to ~1800 m for the range crests in the main half graben.

It is probably accidental that these values are so similar to those in Fig. 8. Even allowing for uncertainty in θ and ϕ, the model in Fig. 9(b) is unrealistic in several ways. The vertical movements are modified by sediment loading (Jackson *et al.* 1988), which may be three-dimensional on these length scales, and by erosion. The faulting in the region where the half grabens change polarity is not as simple as illustrated in Fig. 9(b): the faults are probably not all parallel with the same dip and tilt, and some faults dip the other way, breaking up the coherence of the tilted blocks. The virtue of the model in Fig. 9(b) is that it is simple. It allows an order-of-magnitude estimate of the relative elevation between the basement ridge and the adjacent large half graben. It also draws attention to two effects: (i) basement highs are expected in regions where the main faults change polarity if the amount of extension across them is the same as in the adjacent half graben; and (ii) the widest half graben should also be the deepest. The implications of these effects are important. Intra-basin highs are potential barriers to axial drainage, depending on whether sedimentation in the main half graben is able to keep pace with the relief created by faulting. Pleasant Valley is both narrower (~8 km) and at higher elevation (~1340 m) than northern Dixie Valley (~20 km wide and ~1066 m elevation), suggesting that the sedimentation rate in Dixie Valley is insufficient to eliminate the difference in elevation between it and Pleasant Valley. In pluvial Late Lahontan times, the highest lake shorelines in Dixie Valley (which formed an isolated lake) were at only 1100 m elevation (Mifflin & Wheat 1979), well below the elevation of Pleasant Valley. Thus three possible reasons for Spring Creek draining south into Dixie Valley rather than internally into Pleasant Valley are: (a) sedimentation in Pleasant Valley was always sufficient to keep it filled to the level of the basement ridge so that axial drainage could reach Dixie Valley;

(b) the axial drainage of Pleasant Valley was captured by Dixie Valley; and (c) Spring Creek is the descendant of a south-flowing antecedent stream that formed before the onset of the present faulting.

The incision of Wood Canyon into the hanging wall of the Pearce scarp is related to the behaviour of Spring Creek. Spring Creek has a gentle gradient in central Pleasant Valley, losing only 90 m in height over 25 km along the main stretch of the Pearce scarp (between points A (1400 m) and B (1310 m) on Fig. 7). Over the 11 km between point B (Fig. 7) and the narrow gorge cut in Triassic limestones at C (elevation ~1195 m) through which it enters northern Dixie Valley, Spring Creek drops ~120 m and has incised the alluvial sediments through which it flows. The gentle slope of Spring Creek in central Pleasant Valley, and its incision in the south suggests that it may have been captured from the south, though some of the incision may be because it flows in the uplifting footwall of the Sou Hills scarp. The lowering of Spring Creek has also caused marked incision of its tributaries (Fig. 4). The tributaries are mostly incised only into the toes of the alluvial fans where they meet Spring Creek, presumably because the discharge from these streams is minor or the incision has not operated for long. Only Wood Canyon itself has incised deeply all the way up to the Pearce scarp, probably a consequence of its much greater discharge and catchment area than the other streams.

PLEASANT VALLEY: NORTHERN END

At the northern end of Pleasant Valley both the Pearce and Tobin fault scarps closely follow their respective range fronts (Fig. 6). The 1915 surface rupture at the northern end of the Pearce scarp dies out as the topography in its footwall dies out. The southern end of the 1915 ruptures on the Tobin scarp overlap the 1915 Pearce scarp ruptures by about 2 km. The morphological expression of the Tobin fault segment continues 4–5 km south of the 1915 ruptures, but this part of the Tobin fault did not break the surface in 1915 (Wallace 1984a) (Fig. 10).

The drainage in the overlap of the Pearce and Tobin scarps is quite unlike what is expected in the simple cartoon of Fig. 1. There is no drainage flowing parallel to the strike of the fault segments, making use of the along-strike gradient as it passes from the footwall of one segment to the hanging wall of the next, nor is there a single large stream and drainage basin analogous to Wood Canyon farther south. Instead all the streams here have small elongate drainage basins and flow perpendicular to strike (Figs. 6, 7 and 10). North of the overlap is a regular bajada surface (see Wallace 1978a) that, farther south, is uplifted into the region of the overlap itself (Fig. 11). In the northern part of the bajada, north of the Pearce scarp and adjacent to the Tobin scarp, the streams are not incised, except locally

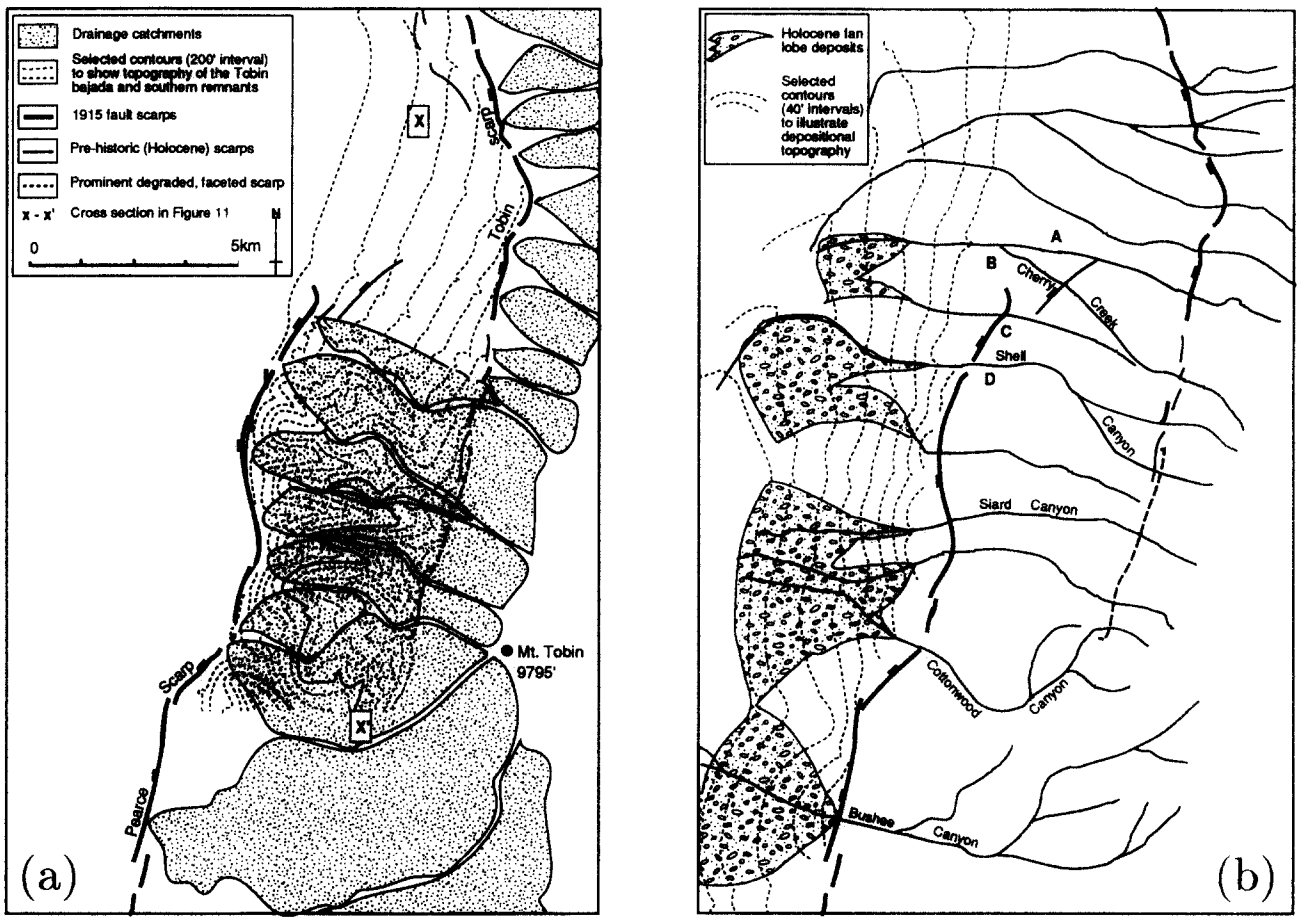

Fig. 10. (a) & (b) Detailed maps of the region where the Pearce and Tobin fault segments overlap (see Fig. 7 for location).

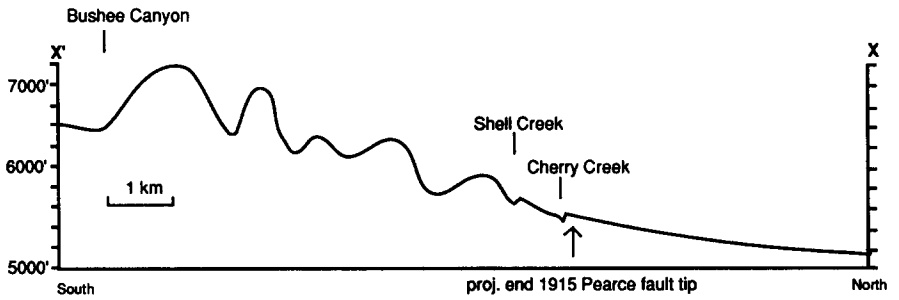

Fig. 11. Cross-section parallel to strike in the overlap between the Pearce and Tobin fault scarps (see Fig. 10a for location).

at their heads. However, the two streams immediately north of the Pearce scarp itself (the north and south forks of Cherry Creek, marked A and B in Fig. 10) are markedly incised *in the hanging wall of the Tobin scarp* to a point about 500 m west of the projected continuation of the Pearce fault segment. Recall that nowhere else (except for the obviously special circumstances of Wood Canyon) does fan incision occur in the immediate hanging walls of faults. The streams crossing the Pearce scarp itself show a clear progression from north to south. All streams in the footwall are deeply incised. The two northernmost streams (C and D in Fig. 10) have previously-incised channels in the hanging wall that are now depositional and infilling (Fig. 6b). Farther south in the hanging wall of the Pearce fault segment the channels feed alluvial fans with limited fan head incision, which become progressively larger and eventually coalesce.

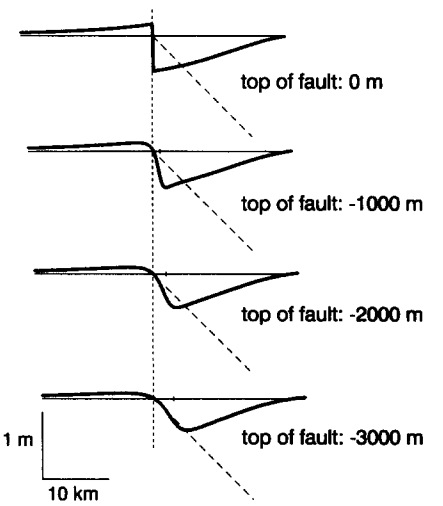

Fig. 12. Cross-sections to illustrate the surface deformation (thick line) associated with slip on a buried normal fault (dashed line). The surface deformation is vertically exaggerated (see 1 m scale bar), but the normal fault is shown at its true dip of 45°. The bottom of the normal fault is at 15 km, but the top varies from 0 m (cutting the surface) to −3000 m (3 km depth). Profiles are calculated for uniform slip of 1 m on an infinitely long fault embedded in an elastic half space, and are aligned where the fault projects to the surface. The calculations obviously represent a gross simplification of the situation at the end of the Pearce fault segment, but illustrate the general principal: as the fault is buried, the discontinuity at the surface (top profile) changes to a monocline, and the point of maximum subsidence migrates into the hanging wall.

Fault growth?

Our preferred interpretation of these observations is as follows. The streams in the hanging wall of the Tobin scarp immediately north of the northernmost 1915 ruptures on the Pearce scarp are incised because they are being uplifted as a result of slip on the buried northward continuation of the Pearce fault segment. Since displacement contours on faults, including the zero displacement contour or tip line, are often approximately elliptical (e.g. Gibson *et al.* 1989, Walsh & Watterson 1989), it is probable that, at depth, the 1915 rupture on the Pearce segment continued a little northward of the surface ruptures without breaking the surface. The surface deformation above this buried part of the fault is a slope or monocline rather than a discontinuity, and stream incision continues slightly into the hanging wall of the projected Pearce fault (Figs. 6 and 10). We have insufficient data to calculate true displacement contours on the Pearce fault, but the effect of the monocline above a buried fault is illustrated in Fig. 12. As the top of the fault (the zero-displacement contour) becomes deeper, the lowest point on the subsiding valley floor migrates into the projected hangingwall; so does the point of inflection on the monocline gradient, which is roughly the point to which incision of the drainage will occur.

We think the northern tip of the Pearce fault segment is propagating northward (see also Cowie & Scholz 1992b). As it does so, the surface ruptures also propagate north and cut the monocline. The uplift in the projected hanging wall now becomes subsidence in the actual hanging wall, and the incised channel begins to aggrade, while the part of the stream that remains in the footwall incises deeply. As the Pearce fault propagates north in this way it uplifts the bajada, incorporating it into the footwall and causing the inherited streams to downcut rapidly. This evolution is illustrated in Fig. 13, and will lead to the topographic profile in Fig. 11, in which the old bajada surface is recognizable as the ridge crests between the streams in the footwall of the Pearce fault. The dominance of the effects of the Pearce fault segment suggests that the Tobin fault segment is less important in the region of the overlap: i.e. that it moves less frequently or that its active southern tip is migrating northwards.

The sequence of events described above explains the drainage observations in a simple way and is consistent with the important geological observation that the 1915 ruptures on the Tobin fault do not extend as far south as the pre-1915 surface ruptures (Wallace 1984a), which in

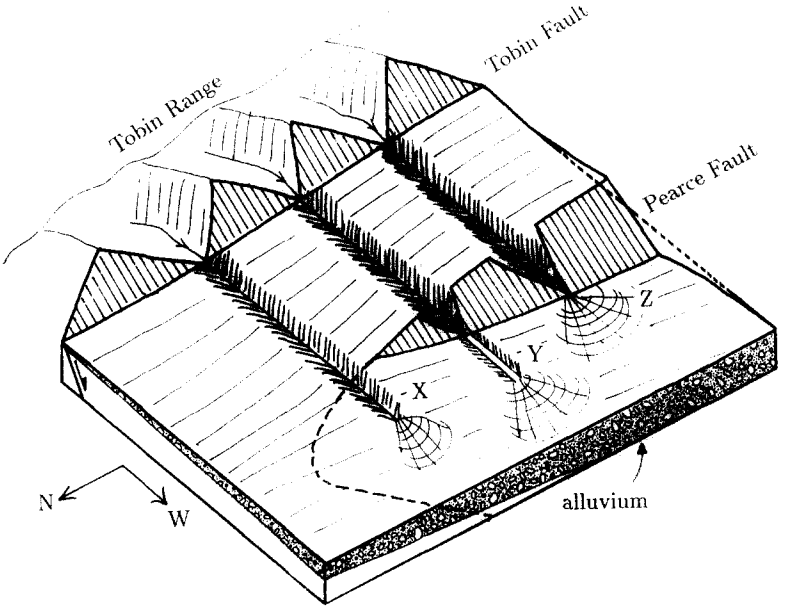

Fig. 13. Sketch of stream and fan evolution in the region where the Pearce and Tobin fault segments overlap. The dashed line indicates that the edge of the Pearce fault continues underground north of where it terminates at the surface. Streams X, Y and Z are all incised in the hanging wall of the Tobin fault. Stream X is also incised a few hundred metres into the projected hanging wall of the Pearce fault (i.e. beyond where it terminates at the surface) and produces a depositional lobe where incision ceases. Stream Y was once incised, but now is depositional and has a flat bottom in the hanging wall of the Pearce fault. It produces a depositional lobe at the end of the originally incised channel. Stream Z has constructed a fan adjacent to the fault scarp, presumably having buried the earlier stages in its evolution represented by streams X and Y. Compare with the view in Fig. 6(b).

turn do not extend as far south as the morphological expression of the fault.

One other feature of the drainage system might be related to the northward propagation of the Pearce fault segment. Halfway along the Pearce scarp are two abnormally large catchments feeding Golconda Canyon and Bushee Creek (Figs. 6 and 7). Both catchments are several times larger than those feeding the other canyons that cross the Pearce scarp. Their large size may be related to the rock type in their hinterland, which is partly Tertiary andesite rather than the Ordovician greenstones, cherts and argillites to the north and the Triassic carbonates to the south. Another possible explanation for their large size is that they originated as major stream systems flowing round the ends of the Tobin and Pearce faults, before the Pearce segment began to propagate northwards (Fig. 14). If this were so, the original Pearce segment would have been about 15 km long, rather than the 30 km it is now. This is not a strong argument, but is a plausible consequence of the northward propagation of the Pearce scarp, for which the evidence is more convincing.

Table 1. The number of earthquakes (N) and the incremental increase in fault length (δL) per earthquake associated with a 10 km increase in length of the northern end of the Pearce fault. Estimates are based on the uplifted bajada surface or theoretical growth models of Cowie & Sholz (1992b) and Walsh & Watterson (1988)

	N	δL (m)
Bajada surface	200–300	50–30
Cowie & Scholz (1992b)	270	45
Walsh & Watterson (1988)	222–444	45–23

Assuming our hypothesis that the Pearce fault segment has propagated north is correct, we can say little about its likely rate of propagation. The bajada surface that is uplifted between the Pearce and Tobin scarps is of unknown age: in Nevada such features may be up to a million or more years old (Wallace 1978a). We may make an approximate minimum estimate for the age of the bajada on the west side of the Tobin scarp as follows. The mean Holocene deposition rate in the area is around

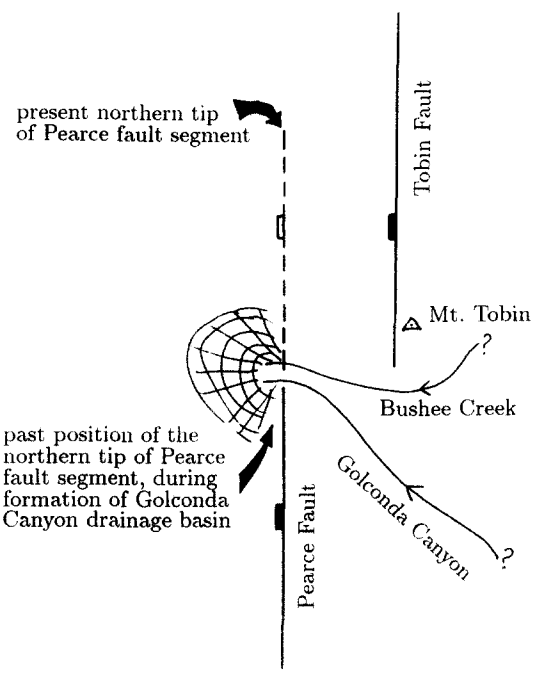

Fig. 14. Sketch showing the hypothetical positions of Golconda Canyon and Bushee Creek before northward propagation of the Pearce fault segment.

0.05 mm year^{-1}, estimated from the thickness of piedmont sediments (Wallace 1984a,b) that overlie the 6850 year old Mazama ash (Bacon 1983). There are at least 20 m of alluvium overlying bedrock in the incised parts of the bajada, indicating a minimum age of around half a million years for construction of the depositional surface. At the southern end of the profile in Fig. 11 the bajada is uplifted about 600 m. This uplift would require about 200–300 earthquakes similar to the 1915 event on the Pearce fault (assuming that movement on the adjacent Tobin fault has no counter-effect), during which time the Pearce fault propagated about 10 km. In other words, the propagating tip of the Pearce fault segment would advance about 50 m in each earthquake. The average return time of earthquakes on the Pearce segment is not known, but from limited trenching is probably measured in thousands (Bonilla *et al.* 1984) or even tens of thousands of years (Machette, personal communication 1992), so that 200–300 earthquakes could require at least 1–2 million years to occur, and the propagating tip would travel at an average velocity of up to ~1 cm year^{-1}. Alternatively, we can attempt to estimate time scales from regional considerations. If the long-term slip rate on the fault is $\dot{u}$, and the approximate slip in each earthquake is $\bar{u}$, then the time needed for N earthquakes to occur is $\bar{u}N/\dot{u}$. The total extension rate across the Basin and Range Province is the order of 10 mm year^{-1} (Minster & Jordan 1987), some of which occurs on the eastern (Wasatch) and western (Sierra Nevada) margins. Probable long-term slip rates on the Central Nevada Seismic Belt faults are the order of 1 mm year^{-1}, so that if $\bar{u}$ is ~3 m (Wallace 1984a) then 300 earthquakes would require about 900,000 years to occur. This analysis is speculative, and contains a number of assumptions that are questionable. The most important is that the Pearce fault segment moves in 'characteristic' earthquakes (i.e. the whole fault moves at once, and not portions of it in smaller earthquakes) that occur regularly rather than cluster in time. Such estimates of propagation rates or fault growth in each earthquake are only likely to be good to an order of magnitude, at best. Nonetheless, they seem to us to be reasonable. For instance, the end of the 1915 surface rupture on the Pearce scarp is roughly coincident with the end of the topographic expression of the pre-existing fault: one is not obviously (by more than about 200 m) in front of or behind the other. A propagation rate of around 50 m per earthquake would produce this effect (i.e. be difficult to recognize on the ground): a rate that was an order of magnitude greater would be easily recognizable. In the next section we compare these estimated growth rates with theoretical models of fault growth.

The most important feature of this locality is that the Pearce fault segment produces uplift that is sufficiently rapid for the streams in its footwall to incise rather than make use of the natural slope parallel to strike (Fig. 11) as would be expected in an en échelon fault step (Fig. 1). This observation requires the streams crossing the Pearce scarp to be antecedent, and suggests that in the region of the fault step the Pearce scarp is younger than the Tobin scarp. In this sense the Pearce fault has propagated into this region. However, can we distinguish an incremental northward propagation of the northern tip of the Pearce fault (as we have assumed above) from the steady *in situ* increase in total displacement of the Pearce fault segment north of Golconda Canyon without a change of length? Our interpretation that the fault tip propagates northwards relies on the progression, from north to south along the Pearce scarp of: (i) incised stream channels (A and B in Fig. 10) in both the projected footwall and hanging wall sides, ahead of the surface outcrop of the tip of the fault; (ii) previously-incised stream channels (C and D in Fig. 10), *which are now depositional and infilling*, in the hanging wall of the Pearce scarp surface rupture at its northernmost end; and (iii) the growth of alluvial fans and presumed burial of the once-incised channels farther south. We interpret these observations as resulting from the incremental propagation of the surface rupture on the Pearce fault northwards. Were it not for these observations, it would be difficult to distinguish our hypothesis that the northward tip propagates from the hypothesis that the fault grows in total displacement without any change in length. An interesting feature of Figs. 6(a) and 10 is that the two streams immediately north of the Pearce scarp, which are incised into the bajada, are convex towards the north, suggesting that they may have migrated and incised in response to deformation at the fault tip. This is compatible with both hypotheses outlined above, but if the streams south of the fault tip are also convex northwards, this would favour the propagating fault tip hypothesis. There are only five major streams that flow from the Tobin scarp directly across the Pearce scarp (Fig. 6a) and the three northern ones are all convex towards the north, but we do not think the signal so clear as to be conclusive.

Growth at the southern end of the Pearce fault

The situation at the southern end of the Pearce fault segment (Fig. 4) resembles in some ways that at the northern end. The 1915 faulting extends south beyond Wood Canyon, with streams in its footwall that are incised across the piedmont in the hanging wall of an apparently less active fault (marked F in Fig. 4a) to the east. The hanging wall of this less active scarp (F) consists of coalesced alluvial fans, but with a less regular surface than the bajada at the north end of the Pearce fault. The incision of these fans suggests that the Pearce fault segment is more active than the fault (F) in the east, and may have propagated south from a previous termination at Wood Canyon.

DISCUSSION

Compatibility with growth models

Several recent studies have addressed the problem of fault growth (e.g. Watterson 1986, Walsh & Watterson

1988, Cowie & Scholz 1992a,b,c, Gillespie *et al.* 1992). All agree that some relation exists between the maximum displacement D on a fault and its length L, of the form $D \propto L^n$, though they differ on the value of n. By selecting observations of D and L over several orders of magnitude, Watterson (1986) proposed that $D \propto L^2$ whereas Marrett & Allmendinger (1991) and Gillespie *et al.* (1992) suggested that $D \propto L^{1.5}$. Cowie & Scholz (1992c) suggested that $D \propto L$, but also that the relationship for large faults (which penetrate the entire upper seismogenic crust) may differ from that for smaller faults. Cowie & Scholz (1992b) also present a theoretical model of fault growth supporting their belief that $n = 1$. Whatever the true value of n, it is because a relationship of this sort exists that as a fault grows in displacement by repeated earthquakes it should also grow in length: there is no observational or theoretical basis for suggesting that *in situ* increase of displacement without accompanying increase in length is an important process.

Differing models exist to describe the growth in fault length. Watterson (1986) and Walsh & Watterson (1988) proposed an empirically-derived arithmetic growth law to explain their non-linear relationship between D and L, in which displacement increases by a constant amount in each earthquake, independent of fault length. By contrast, Cowie & Scholz (1992b) derived a growth law from arguments based on fracture mechanics in which the increase in displacement is linearly related to fault length: this law is compatible with $n = 1$ but not with $n = 2$. In the previous section we used the uplifted bajada surface at the northern end of the Pearce fault segment (Fig. 11) to estimate that this fault is growing at a rate of about 50 m per earthquake, and has taken about 200–300 earthquakes (and possibly 1–2 million years) to propagate 10 km. It is instructive to compare these estimates with growth rates predicted from theoretical models.

Cowie & Scholz (1992b) give an expression (their equation 22) indicating the number of earthquakes (N) required to increase the length of a fault from an initial value L_0 to a length L:

$$N = \frac{\log L/L_0}{\log (1 + \alpha/\gamma)}, \tag{1}$$

where α is the ratio of the mean slip during an earthquake to the rupture length and γ is the ratio of the mean accumulated displacement on a fault to its length. The ratio $r = \alpha/\gamma$ is the proportional increase in fault length during each earthquake. The expected value of α is about 5×10^{-5} for continental earthquakes (Scholz 1982), and the expected value of γ for faults of length ~30 km is $\sim 10^{-2}$ (fig. 3 of Cowie & Scholz 1992c, assuming that mean displacement is about half the maximum displacement). The ratio r is then $\sim 1.5 \times 10^{-3}$ or 0.15%: thus the Pearce fault segment, currently ~30 km long, would be expected to grow by 45 m per earthquake. If we consider the propagation of the last 10 km of the northern end of the Pearce scarp (Fig. 11), then $L/L_0 \sim 3/2$, and the expected number of earthquakes required to achieve this growth is 270. The closeness of these numbers to our predictions using the uplifted bajada surface is fortuitous: they are critically dependent on the value of r. However, if we take the observed value of 10×10^{-5} for α on the Pearce scarp in the 1915 earthquake (i.e. 3 m displacement over 30 km length: Wallace 1984a), and estimate the maximum throw (D) on the Pearce fault from the elevation of the footwall (~1000 m) and the thickness of sediments in the hanging wall (also ~1000 m from gravity measurements: Fig. 8 and Fonseca 1988), so that $\gamma \sim 6.7 \times 10^{-2}$, then r is unchanged at 1.5×10^{-3} or 0.15%. The increment of growth in the last earthquake and the number of earthquakes necessary for the 10 km growth also remain unchanged.

In Walsh & Watterson's (1988) arithmetic growth model, the increment of slip a between successive earthquakes is given by (their equation A3):

$$a = \frac{u_n^2}{2D}, \tag{2}$$

where u_n is the slip in the last earthquake and D is the maximum displacement on the fault. If we take $u_n = 3$ m in the 1915 earthquake and $D = 2$ km (from above), then $a = 2.25$ mm. The number of earthquakes (N) required for the fault to grow from length L_0 to L is:

$$N = \frac{\alpha}{a}(L - L_0). \tag{3}$$

If we take the expected value for α of 5×10^{-5} (Scholz 1982), then the number of earthquakes required to propagate the fault 10 km is 222. Using the observed value of 10×10^{-5} for α from the 1915 earthquake increases this number of earthquakes to 444. The incremental increase in fault length per earthquake is a/α, i.e. 45 m if $\alpha = 5 \times 10^{-5}$ or 23 m if $\alpha = 10 \times 10^{-5}$. Once again these numbers are similar to the estimates obtained earlier from the uplifted bajada surface.

The two theoretical growth models of Walsh & Watterson (1988) and Cowie & Scholz (1992b) give similar estimates for propagation rates at the northern end of the Pearce scarp to those obtained from the uplifted bajada surface in Fig. 11, in which we simply assumed that earthquakes repeated with an average displacement of about 3 m, as in 1915. Our assumption of a constant displacement in each earthquake is a simplification: we expect the average displacement to have increased as the fault grew, from ~2 m when the fault was 20 km long to the ~3 m observed in 1915. But this effect does not change our estimate that 200–300 earthquakes were needed to uplift the bajada surface. These estimates are all compared in Table 1, but the reader should not be misled by their apparent close agreement: they agree to an order of magnitude, but all are very dependent on their conceptual models and the values chosen for α, γ and D. The only important difference between them is that the theoretical models of Walsh and Watterson (1988) and Cowie & Scholz (1992b) predict how faults the size of Pearce fault segment should grow, whereas the estimate from the uplifted bajada is based, albeit

naively, on observations. Clearly, there is nothing in the observations we have presented that favours one theoretical model over another.

Episodic fault activity and growth

Suppose the Pearce fault segment has indeed grown from a position in which its northern end was at Golconda Canyon and its southern end was at Wood Canyon. These large canyons and drainage basins were then located at fault segment terminations, in a situation that resembles the sketch in Fig. 1. The size of these catchments relative to the others suggests that their structural position was fixed for some time. This implies that the Pearce fault segment may have grown episodically and that periods of quiescence occurred during which the large drainage systems at the fault terminations became established. Fault growth and propagation may then have taken place quite rapidly, producing the portion of the Pearce fault north of Golconda Canyon in only 1–2 Ma. The deep canyons at the former fault terminations have not been able to change their courses in response to renewed vertical motions and tilting, and kept their position as the fault terminations propagated past them. The notion that the faulting occurs in episodes that switch from one locality to another in the Basin and Range is not new: it was proposed by Wallace (1978a, 1984b, 1987, 1989), partly to account for variations in the appearance of fault-bounded range fronts, Thus large canyon systems between fault segments (as in Fig. 1) may indicate that those faults have experienced a period of inactivity. If fault activity were to cease at the northern end of the Pearce segment, the natural slope along strike between the Pearce and Tobin scarps (Fig. 11) will presumably lead to capture of the existing drainage basins and formation of a single big canyon similar to Wood Canyon.

If the Pearce scarp has grown from an initial length between Wood and Golconda Canyons, it has grown more to the north (12 km) than to the south (6 km). Simple theoretical models imply a symmetric growth of the fault surface, but this is not necessarily required by observations of displacement contours on fault surfaces, which sometimes display asymmetry (e.g. Walsh & Watterson 1989, Gibson *et al.* 1989). Propagation of the southern end of the Pearce fault may be inhibited by entering a zone of distributed faults that accommodates a change in the polarity of the major half graben.

CONCLUSIONS

It is clear that the vertical motions and tilting that accompany normal faulting must influence the drainage in faulted regions. Axial drainage between basins may be controlled by basin width: in simple half-graben terrains the deepest basins should also be the widest. Basins that are adjacent along strike may be separated by transverse basement highs for the simple reason that the distributed minor faulting where faults step en échelon or change polarity generates less relief between footwalls and hangingwalls than do the single major faults that bound the main half graben. Whether the axial drainage will be able to pass the transverse basement barriers, and hence determine whether the basin will be a net source or a sink of sediments, will depend on whether the sediment flux itself is able to maintain the valley floor to the height of the sill.

En échelon steps between fault segments are often the sites of major drainage basins and alluvial fans. In northern Pleasant Valley, where this is *not* the case, we argue that it is because one fault segment is growing in length faster than the drainage is able to respond. At the southern end of Pleasant Valley, Wood Canyon issues from a prominent fault step, but the 1915 surface ruptures continued beyond it, perhaps indicating a southward growth of the Pearce fault segment. These large canyons and their catchments presumably take time to form, and may do so in periods of relative inactivity. Thus whether we currently see a large drainage system in a fault step may depend on the current state of activity on the fault system. In Pleasant Valley we may be witnessing a spectrum of fault activity indicated by drainage development: from the Pearce–Tobin segment overlap in the north (a rapidly growing fault), through Wood Canyon in the south (more recently or slowly growing), to Golconda Canyon in the centre of the Pearce segment (formed during a period of quiescence at what was then the fault termination, but now left behind by the rapidly propagating Pearce segment). The rate of fault growth we estimate from the uplifted bajada surface at the north end of the Pearce fault segment is about 50 m per earthquake. This is similar to predicted growth rates from theoretical models, but is too imprecise to distinguish between these models.

We conclude that potentially useful structural information is preserved in the drainage associated with active fault systems. This information is mostly qualitative because of the paucity of dateable material. Nonetheless, drainage evolution may provide clues to episodic fault activity and growth that are difficult to obtain by more conventional geological means.

Acknowledgements—J. A. Jackson thanks the Dean of the School of Earth Sciences at Stanford University for support while this work was carried out. This study was partially supported by NERC, Sun Oil, Shell International and Amerada Hess. We thank R. Arrowsmith, J. W. Bell, W. Bull, P. Cowie, B. Deffontaines, M. Machette, A. Smith, S. Treagus and an anonymous referee for helpful reviews that improved the final manuscript, K. Priestley for help in the field and R. E. Wallace for permission to reproduce his photographs. We are especially grateful to R. E. Wallace and G. A. Thompson for discussions and guidance on all aspects of the geology of central Nevada, but they do not necessarily agree with the views expressed here. Cambridge Earth Sciences contribution 3360.

REFERENCES

Bacon, C. R. 1983. Eruptive history of Mount Mazama and Crater Lake caldera, Cascade Range, U.S.A. *J. Volc. Geothermal Res.* **18**, 57–115.

Benson, L. V. & Thompson, R. S. 1987. Lake level variation in Lake Lahontan Basin for the past 50,000 years. *Quat. Res.* **28**, 69–85.

Bonilla, M. G., Villalobos, H. A. & Wallace, R. E. 1984. Exploratory trench across the Pleasant Valley fault, Nevada. *Prof. Pap. U.S. geol. Surv.* **1274B**.

Cowie, P. A. & Scholz, C. H. 1992a. Physical explanation for the displacement–length relationship of faults using a post-yield fracture mechanics model. *J. Struct. Geol.* **14**, 1133–1148.

Cowie, P. A. & Scholz, C. H. 1992b. Growth of faults by accumulation of seismic slip. *J. geophys. Res.* **97**, 11,085–11,095.

Cowie, P. A. & Scholz, C. H. 1992c. Displacement–length scaling relationship for faults: data synthesis and discussion. *J. Struct. Geol.* **14**, 1149–1156.

Crone, A. J. & Haller, K. M. 1991. Segmentation and the coseismic behaviour of Basin and Range normal faults: examples from east-central Idaho and south-western Montana, U.S.A. *J. Struct. Geol.* **13**, 151–164.

De Polo, C. M., Clark, D. G., Slemmons, D. B. & Ramelli, A. R. 1991. Historical surface faulting in the Basin and Range province, western North America: implications for fault segmentation. *J. Struct. Geol.* **13**, 123–136.

Dohrenwend, J. C. 1987. Basin and Range. In: *Geomorphic Systems of North America* (edited by Graf, W. L.). *Geol. Soc. Am., Centennial Special Volume* **2**, 303–342.

Doser, D. 1986. Earthquake processes in the Rainbow Mountain–Fairview Peak–Dixie Valley, Nevada, region. *J. geophys. Res.* **91**, 12,572–12,586.

Doser, D. 1988. Source parameters of earthquakes in the Nevada seismic zone, 1915–1943. *J. geophys. Res.* **93**, 15,001–15,015.

Doser, D. & Smith, R. B. 1989. An assessment of source parameters of earthquakes in the Cordillera of the western United States. *Bull. seism. Soc. Am.* **79**, 1383–1409.

Ebinger, C. J. 1989. Geometric and kinematic development of border faults and accommodation zones, Kivu-Rusizi rift, Africa. *Tectonics* **8**, 117–133.

Fonseca, J. 1988. The Sou Hills: a barrier to faulting in the central Nevada Seismic Belt. *J. geophys. Res.* **93**, 475–489.

Gibson, J. R., Walsh, J. & Watterson, J. 1989. Modelling of bed contours and cross-sections adjacent to planar normal faults. *J. Struct. Geol.* **11**, 317–328.

Gillespie, P. A., Walsh, J. J. & Watterson, J. 1992. Limitations of dimension and displacement data from single faults and the consequences for data analysis and interpretation. *J. Struct. Geol.* **14**, 1157–1172.

Harris, J. P. & Fowler, R. M. 1987. Enhanced prospectivity of Mid-Late Jurassic sediments of the South Viking Graben. In: *Petroleum Geology of North West Europe* (edited by Brooks, J. & Glennie, K.). Graham & Trotman, London, 879–898.

Jackson, J. A. & McKenzie, D. P. 1983. The geometrical evolution of normal fault systems. *J. Struct. Geol.* **5**, 471–482.

Jackson, J. A. & White, N. J. 1989. Normal faulting in the upper continental crust: observations from regions of active extension. *J. Struct. Geol.* **11**, 15–36.

Jackson, J. A., Gagnepain, J., Houseman, G., King, G., Papadimitriou, P., Soufleris, C. & Virieux, J. 1982. Seismicity, normal faulting, and the geomorphological development of the Gulf of Corinth (Greece): the Corinth earthquakes of February and March 1981. *Earth Planet. Sci. Lett.* **57**, 377–397.

Jackson, J. A., White, N. J., Garfunkel, Z. & Anderson, H. 1988. Relations between normal fault geometry, tilting and vertical motions in extensional terrains: an example from the southern Gulf of Suez. *J. Struct. Geol.* **10**, 155–170.

Leeder, M. R. & Gawthorpe, R. L. 1987. Sedimentary models for extensional tilt block/half-graben basins. In: *Continental Extensional Tectonics* (edited by Coward, M. P., Dewey, J. F. & Hancock, P. L.). *Spec. Publs. geol. Soc. Lond.* **28**, 139–152.

Leeder, M. R. & Jackson, J. A. 1993. The interaction between normal faulting and drainage in active extensional basins, with examples from the western United States and central Greece. *Basin Research* **5**, 79–102.

Leeder, M. R., Seger, M. J. & Stark, C. P. 1991. Sedimentology and tectonic geomorphology adjacent to active and inactive normal faults in the Megara basin and Alkyonides Gulf, central Greece. *J. Geol. Soc. Lond.* **148**, 331–343.

Lyon-Caen, H., Armijo, R., Drakopoulos, J., Baskoutass, J., Delibassis, N., Gaulon, R., Kouskouna, V., Latoussakis, J., Makropoulos, K., Papadimitriou, P., Papanastassiou, D. & Pedotti, G. 1988. The 1986 Kalamata (south Peloponessus) earthquake: detailed study of a normal fault and tectonic implications. *J. geophys. Res.* **93**, 14,967–15,000.

Machette, M. N., Personius, S. F., Nelson, A. R., Schwartz, D. P. & Lund, W. R. 1991. The Wasatch fault zone, Utah—segmentation and history of Holocene earthquakes. *J. Struct. Geol.* **13**, 137–150.

Marrett, R. & Allmendinger, R. W. 1991. Estimates of strain due to brittle faulting: sampling of fault populations. *J. Struct. Geol.* **13**, 735–738.

Mifflin, M. D. & Wheat, M. M. 1979. Pluvial lakes and estimated pluvial climates of Nevada. *Nevada Bur. Mines Geol.* **94**, 1–57.

Minster, J. B. & Jordan, T. H. 1987. Vector constraints on western U.S. deformation from space geodesy, neotectonics and plate motions. *J. geophys. Res.* **92**, 4798–4804.

Morrison, R. B. 1964. Lake Lahontan: geology of the southern Carson Desert. *Prof. Pap. U.S. geol. Surv.* **401**.

Nosker, S. 1981. Stratigraphy and structure of the Sou Hills, Pershing County, Nevada. M.S. thesis, University of Nevada, Reno.

Roberts, S. & Jackson, J. A. 1991. Active normal faulting in central Greece: an overview. In: *The Geometry of Normal Faults* (edited by Roberts, A. M., Yielding, G. & Freeman, B.). *Spec. Publs. geol. Soc. Lond.* **56**, 125–142.

Rosendahl, B. R., Reynolds, D. J., Lorber, P. M., Burgess, C. F., McGill, J., Scott, D., Lambiase, J. J. & Derksen, S. J. 1986. Structural expressions of rifting: lessons from Lake Tanganyika, Africa. In: *Sedimentation in the African Rifts* (edited by Frostick, L. E., Renaut, R. W., Reid, I. & Tiercelin, J. J.). *Spec. Publs. geol. Soc. Lond.* **25**, 29–43.

Scholz, C. H. 1982. Scaling laws for large earthquakes: consequences for physical models. *Bull. seism. Soc. Am.* **72**, 1–14.

Scholz, C. H., Aviles, C. & Wesnousky, S. 1986. Scaling differences between large interplate and intraplate earthquakes. *Bull. seism. Soc. Am.* **76**, 65–70.

Schwartz, D. P. & Sibson, R. H. 1989. Fault segmentation and controls of rupture initiation and termination. *U.S. geol. Surv. Open-file Rep.* **89-315**.

Shimazaki, K. 1986. Small and large earthquakes: the effects of the thickness of the seismogenic layer and the free surface. In: *Earthquake Source Mechanics* (edited by Das, S., Boatwright, J. & Scholz, C. H.). *Am. Geophys. Un. Geophys. Monogr.* **37**, 209–216.

Slemmons, D. B. 1957. Geological effects of the Dixie Valley–Fairview Peak, Nevada, earthquakes of December 16, 1954. *Bull. siesm. Soc. Am.* **47**, 353–375.

Stewart, J. H. 1980a. Regional tilt patterns of late Cenozoic basin-range fault blocks, western United States. *Bull. geol. Soc. Am.* **91**, 460–464.

Stewart, J. H. 1980b. Geology of Nevada. *Spec. Publ. Nevada Bur. Mines Geol.* **4**.

Susong, D. D., Janecke, S. U. & Bruhn, R. L. 1990. Structure of a fault segment boundary in the Lost River fault zone, Idaho, and possible effect on the 1983 Borah Peak earthquake rupture. *Bull. seism. Soc. Am.* **80**, 57–68.

Thenhaus, P. C. & Barnhard, T. P. 1989. Regional termination and segmentation of Quaternary fault belts in the Great Basin, Nevada and Utah. *Bull. seism. Soc. Am.* **79**, 1426–1438.

Wallace, R. E. 1977. Profiles and ages of young fault scarps, north-central Nevada. *Bull. geol. Soc. Am.* **88**, 1267–1281.

Wallace, R. E. 1978a. Geometry and rates of changes of fault-generated range fronts, north-central Nevada. *U.S. geol. Surv. J. Res.* **6**, 637–650.

Wallace, R. E. 1978b. Patterns of faulting and seismic gaps in the Great Basin province. In: *Methodology for Identifying Seismic Gaps and Soon to Break Gaps* (edited by J. Evernden). *Proc. Conf. VI, U.S. geol. Surv. Open-file Rep.* **78-943**.

Wallace, R. E. 1984a. Fault scarps formed during the earthquakes of October 2 1915 in Pleasant Valley, Nevada, and some tectonic implications. *Prof. Pap. U.S. geol. Surv.* **1274A**, 1–33.

Wallace, R. E. 1984b. Patterns and timing of late Quaternary faulting in the Great Basin province and relation to some regional tectonic features. *J. geophys. Res.* **89**, 5763–5769.

Wallace, R. E. 1987. Grouping and migration of surface faulting and variations in slip rates on faults in the Great Basin province. *Bull. seism. Soc. Am.* **77**, 868–876.

Wallace, R. E. 1989. Fault plane segmentation in brittle crust and anisotropy in loading system. In: *Fault Segmentation and Controls of Rupture Initiation and Termination* (edited by Schwartz, D. P. & Sibson, R. H.). *U.S. geol. Surv. Open-file Rep.* **89–315**, 400–408.

Wallace, R. E. & Whitney, R. A. 1984. Late Quaternary history of the Stillwater seismic gap, Nevada. *Bull seism. Soc. Am.* **74**, 301–314.

Walsh, J. & Watterson, J. 1988. Analysis of the relationship between displacements and dimensions of faults. *J. Struct. Geol.* **10**, 239–247.

Walsh, J. & Watterson, J. 1989. Displacement gradients on fault surfaces. *J. Struct. Geol.* **11**, 307–316.

Walsh, J. & Watterson, J. 1991. Geometric and kinematic coherence and scale effects in normal fault systems. In: *The Geometry of Normal Faults* (edited by Roberts, A. M., Yielding, G. & Freeman, B.). *Spec. Publs. geol. Soc. Lond.* **56**, 193–203.

Walsh, J. & Watterson, J. 1992. Populations of faults and fault displacements and their effects on estimates of fault-related regional extension. *J. Struct. Geol.* **14**, 701–712.

Watterson, J. 1986. Fault dimensions, displacements and growth. *Pure & Appl. Geophys.* **124**, 365–373.

Wheeler, R. L. 1989. Persistent segment boundaries on basin-rangenormal faults. In: *Fault Segmentation and Controls of Rupture Initiation and Termination* (edited by Schwartz, D. P. & Sibson, R. H.). *U. S. geol. Surv. Open-file Rep.* **89-315**, 432–444.

Yielding, G. 1990. Footwall uplift associated with Late Jurassic normal faulting in the northern North Sea. *J. geol. Soc. Lond.* **147**, 219–222.

Zhang, P., Slemmons, D. B. & Mao, F. 1991. Geometric pattern, rupture termination and fault segmentation of Dixie Valley–Pleasant Valley active normal fault system, Nevada, U.S.A. *J. Struct. Geol.* **13**, 165–176.

SG 16:8-B